# Development of a Technique to Assess Snow-Cover Mapping Errors from Space

Dorothy K. Hall, James L. Foster, Vincent V. Salomonson, *Fellow, IEEE*, Andrew G. Klein, and J. Y. L. Chien

***Abstract*—Following the December 18, 1999, launch of the Earth Observing System (EOS) Terra satellite, daily snow-cover mapping is performed automatically at a spatial resolution of 500 m, cloud-cover permitting, using moderate resolution imaging spectroradiometer (MODIS) data. This paper describes a technique for calculating global-scale snow mapping errors and provides estimates of Northern Hemisphere snow mapping errors based on prototype MODIS snow mapping algorithms. Field studies demonstrate that under cloud-free conditions, when snow cover is complete, snow mapping errors are small ($<$ 1%) in all land covers studied except forests, where errors are often greater and more variable. Thus, the accuracy of Northern Hemisphere snow-cover maps is largely determined by percent of forest cover north of the snowline. From the 17-class International Geosphere-Biosphere Program (IGBP) land-cover maps of North America and Eurasia, we classify the Northern Hemisphere into seven land-cover classes and water. Estimated snow mapping errors in each of the land-cover classes are extrapolated to the entire Northern Hemisphere for areas north of the average continental snowline for each month. The resulting average monthly errors are expected to vary, ranging from about 5–10%, with the larger errors occurring during the months when snow covers the boreal forest in the Northern Hemisphere. As determined using prototype MODIS data, the annual average estimated error of the future Northern Hemisphere snow-cover maps is approximately 8% in the absence of cloud cover, assuming complete snow cover. Preliminary error estimates will be refined after MODIS data have been available for about one year.**

***Index Terms*—Moderate resolution imaging spectroradiometer (MODIS), satellites, snow cover, snow mapping.**

## I. Introduction

Weekly snow-cover maps have been produced of the Northern Hemisphere using visible and near-infrared satellite data since 1966 [1]. In addition, passive-microwave data have been used to produce snow-cover and snow-depth maps of the Northern Hemisphere [2], [3]. While it has been recognized that snow maps are more accurate in some land covers than in others [3], there has been no attempt to assess the accuracy of the maps in individual land covers and to use that information to assess hemispheric or global-scale errors. The need for error assessment is heightened by the 1999 launch of the Terra satellite by the National Aeronautics and Space Administration (NASA), Washington, DC, on which the moderate resolution imaging spectroradiometer (MODIS) sensor is flown. MODIS data are used to produce daily, global snow-cover map products at a spatial resolution of 500 m. Other products are also available. The users of these snow maps require knowledge of the errors inherent in the snow mapping. This paper presents a technique for assessment of the errors of the hemispheric-scale MODIS snow-cover maps.

An algorithm has been developed to map global snow cover using MODIS data. Prototype algorithms have been applied to the Landsat thematic mapper (TM) and the advanced very high resolution radiometer (AVHRR) satellite data from the National Oceanographic and Atmospheric Administration (NOAA), Washington, DC, and MODIS airborne simulator (MAS) data to simulate snow cover mapping with MODIS data. Detailed studies of the prototype at-launch MODIS snow mapping algorithms have been conducted in several different land covers, and associated errors have been determined [4], [5]. Early results using actual MODIS data have provided similar results.

In this work, the Earth's land surface has been classified into seven land-cover classes and water. Using the percentage of each land-cover class north of the position of the average monthly continental snowline, we have estimated average monthly snow mapping errors for North America and Eurasia, for individual land-cover classes.

The inability to map snow cover through dense forests is an important limitation to snow-cover mapping from space. For the purposes of this paper, this limitation is considered in the error estimates. Not considered are the limitations on mapping snow cover using MODIS during darkness and through cloud cover.

Knowledge of the errors of hemispheric-scale snow-cover maps is important because MODIS snow cover products will be used as input to snowmelt-runoff models [6] and general circulation models (GCMs) [7]. Errors of the input products must be known to establish the errors of the output products.

## II. Background

### A. Description of MODIS and the Primary Snow-Cover Mapping Products

NASAs Terra spacecraft was launched into a sun-synchronous, near-polar orbit with a 10:30 a.m. equatorial-crossing time on December 18, 1999. Its five scientific instruments, including the MODIS, permit monitoring of the energy exchanges among the atmosphere, oceans, and land [8].

MODIS is a 36-band spectroradiometer covering visible, near-, shortwave-infrared, and infrared bands from 0.4–14 $\mu$m

Manuscript received May 31, 1998; revised November 16, 2000.

D. K. Hall and J. L. Foster are with NASA/Goddard Space Flight Center, Greenbelt, MD 20771 USA (e-mail: dhall@glacier.gsfc.nasa.gov).

V. V. Salommonson is with NASA/Goddard Space Flight Center, Greenbelt, MD 20771 USA.

A. G. Klein is with the Department of Geography, Texas A&M University, College Station, TX 77843-3147 USA.

J. Y. L. Chien is with the General Sciences Corporation, Laurel, MD 20707 USA.

Publisher Item Identifier S 0196-2892(01)01164-0.

[9]. A swath of data covers an area 2330 km across track and 10 km along track (at nadir). The spatial resolution of the MODIS data ranges from 250 m to 1 km. Among the key land-surface objectives are to map global vegetation and land cover, global land-surface change, vegetation properties, surface albedo, surface temperature, and snow and ice cover daily or every other day [10]–[12].

The MODIS snow mapping algorithm maps global snow cover, cloud-cover permitting, at 500-m spatial resolution using MODIS data [5], [13], [14]. MODIS snow and ice data products are archived at and distributed by the National Snow and Ice Data Center (NSIDC), Boulder, CO [15] beginning in the summer of 2000.

Each MODIS pixel is mapped as snow, cloud, or "other." The MODIS cloud mask at 1-km resolution, developed at the University of Wisconsin, Madison, [16], is input to the snow mapping algorithm. The snow mapping algorithm [5], which has evolved over time, will include subpixel snow cover information.

### *B. Validation of the MODIS Global Snow Mapping Algorithm*

The MODIS-derived Northern Hemisphere snow maps are being compared extensively with other hemispheric-scale maps such as the Northern Hemisphere weekly snow-cover maps produced by the National Environmental Satellite, Data and Information Service (NESDIS), Suitland, MD, and regional-scale 1-km resolution National Operational Hydrologic Remote Sensing Center (NOHRSC) snow maps, Chanhassen, MN, [17]. MODIS maps will also be compared with maps derived from passive-microwave data [2], [18]. These comparisons reveal only relative error because the absolute errors of the NESDIS, NOHRSC, and passive-microwave snow maps have not been established. At local scales, MODIS snow-cover maps will be compared with snow-cover maps derived from the Landsat-7 enhanced thematic mapper plus (ETM+) and Terra's advanced spaceborne thermal emission and reflection radiometer (ASTER) data, at a spatial resolution of up to 15 m.

### *C. Prototype Instruments*

The TM, a near-nadir viewing sensor, $\pm 7.5°$, was first carried on the Landsat-3 satellite in 1982 with a 16-day repeat cycle. It provides 30-m pixel resolution images of the Earth's surface in seven spectral bands, ranging from the visible to the thermal-infrared parts of the spectrum. A TM scene represents an area of $185 \times 185$ km on the ground. The MODIS prototype algorithm for TM uses TM bands 2 (0.52–0.60 $\mu$m), 4 (0.76–0.9 $\mu$m) and 5 (1.55–1.75 $\mu$m).

The MAS acquires imagery in 50 channels ranging from the visible to the thermal-infrared parts of the spectrum (0.527–14.35 $\mu$m), but the MODIS prototype algorithm uses only MAS channels 1–9 (Table I). The MAS collects image data with a ground resolution of 50 m from 20 000-m altitude, and has a cross-track scan width of 85.92°, giving a total field of view of 37.25 km on the ground [19].

TABLE I
SPECTRAL RANGE OF THE MODIS AIRBORNE SIMULATOR (MAS), CHANNELS 1–9

| Channel | Spectral Range |
|---|---|
| 1 | 0.527-0.571 |
| 2 | 0.631-0.684 |
| 3 | 0.683-0.725 |
| 4 | 0.725-0.766 |
| 5 | 0.765-0.807 |
| 6 | 0.806-0.848 |
| 7 | 0.848-0.891 |
| 8 | 0.893-0.926 |
| 9 | 0.924-0.970 |

TABLE II
THE LAND-COVER CLASSES THAT WERE DERIVED FROM THE 17-CLASS IGBP MAPS ARE GIVEN. LAND-COVER CLASSES (SUBCLASSES) THAT COMPRISE EACH OF THE EIGHT CLASSES ARE SHOWN IF APPLICABLE

| Land-cover class | Land-cover sub-class |
|---|---|
| FOREST | Evergreen needleleaf forest<br>Evergreen broadleaf forest<br>Deciduous needleleaf forest<br>Deciduous broadleaf forest<br>Forest |
| MIXED AGRICULTURE AND FOREST | Urban and built-up land<br>Croplands<br>Cropland/natural vegetation mosaic |
| BARREN/SPARSELY VEGETATED | |
| TUNDRA | Woody savannas<br>Savannas |
| GRASSLANDS/SHRUBLANDS | Closed shrublands<br>Open shrublands<br>Grasslands |
| WETLANDS | |
| PERMANENT SNOW AND ICE | |
| WATER | |

### *D. Field Measurements*

An ongoing series of field and aircraft experiments for validation of the MODIS snow algorithm has allowed us to estimate the accuracy of the MODIS prototype snow maps [4], [5] and [13]. Studies of snow-cover mapping accuracy under conditions of complete snow cover in a number of different land covers have been conducted. Simultaneous field and aircraft campaigns have been undertaken in forests and prairies (grasslands) in Saskatchewan [5], agricultural and forested areas in Minnesota and Wisconsin, tundra and forests in northern and central Alaska, and forests in New York and New Hampshire [4], [20]–[23].

A limitation contributing to the reported error is the fact that less snow in forests will be mapped at off-nadir view angles than at nadir. This is because, when viewed from an angle, the tree stems, branches, and trunks block the view of the snow more than when the forest is viewed from nadir. Often, when viewing a snow-covered forest from the air, little or no snow cover will be seen, especially if there is no snow in the tree canopy. The

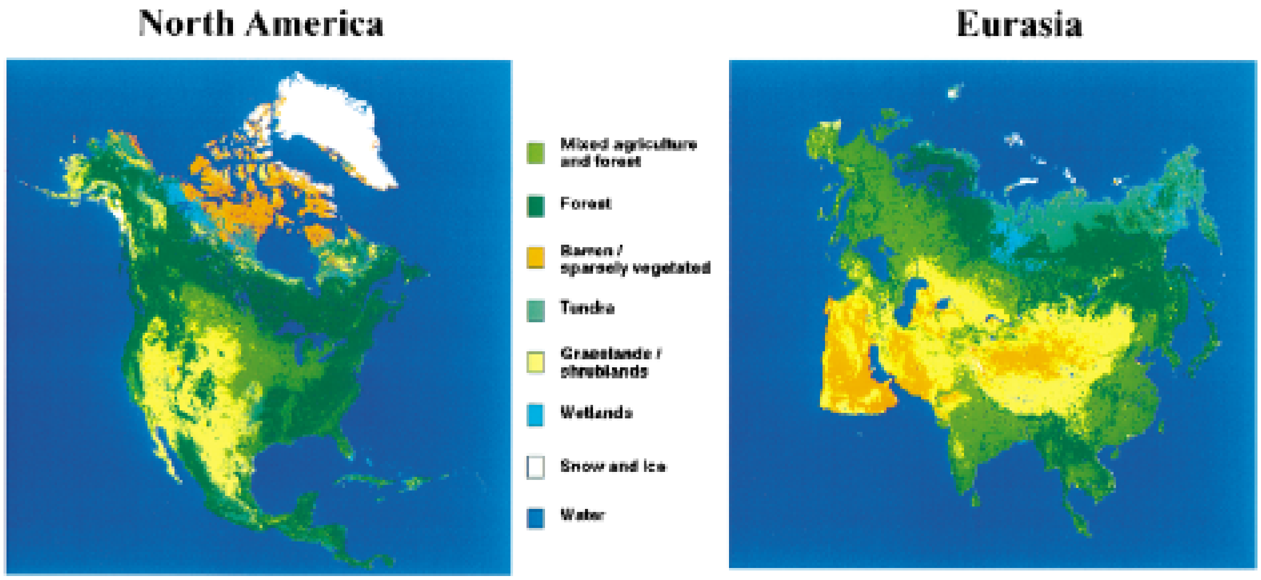


Fig. 1. Land-cover maps (eight classes) of North America and Eurasia derived from the 17-class IGBP map.

prototype studies done using the near-nadir viewing TM sensor have not taken this into account.

## III. Methodology

### *A. Land-Cover Classification*

International Geosphere-Biosphere Project (IGBP) 17-class land-cover maps of North America and Eurasia, developed from 1-km AVHRR data, are used as the base maps for this work. These products are based on monthly normalized difference vegetation index (NDVI) composites from 1992 and 1993 [24]. Since the snow mapping errors are not believed to be vastly different in many of the 17 original IGBP classes, the IGBP maps were modified for this work to encompass only seven common land-cover classes in the Northern Hemisphere (Table II): forest, mixed agriculture and forest, barren/sparsely vegetated, tundra, grasslands/shrublands, wetlands, permanent snow and ice, and water (Fig. 1).

### *B. Determination of Snow Mapping Error Estimates in Forested Areas*

Efforts have been concentrated on determining snow mapping errors in forests. Errors vary with forest-cover density being very low in sparse forests and higher in dense forests, both coniferous and deciduous [4], [5]. The accuracy of snow mapping depends more on the density of tree canopies than on forest type. This has also been shown for passive microwave mapping of snow extent and depth [25], [26].

Snow-cover maps, created using Landsat TM and MAS data for forests in Saskatchewan and central Alaska, have revealed variable accuracies when the MODIS at-launch snow mapping algorithm was employed [4], [5].

In the Saskatchewan study area alone, snow mapping errors range from nearly 0 to 43%, with the highest errors occurring in dense, deciduous forests [5]. However, the errors of snow cover mapping in forests in Saskatchewan as in other forested areas studied, are generally $< 5\%$ [5]. Values reported for the Saskatchewan study area were determined by mapping snow cover using the TM prototype algorithm when snow cover was complete. Areas mapped as non-snow-covered were considered to be in error, as field measurements revealed complete snow cover.

In central Alaska, snow mapping errors in forests were determined by field and satellite measurements, using reflectance as a surrogate measure of vegetation-cover density following the work of Robinson and Kukla [27] and Foster *et al.* [25]. The error associated with snow mapping in the densest vegetation cover in an area of mixed vegetation in central Alaska was 2% [4]. These errors were determined by mapping snow using the MAS under conditions of complete snow cover, as verified by nearly-simultaneous field measurements.

*Forest-Cover Density Maps:* Robinson and Kukla [27], [28] developed a method of estimating vegetation density using Defense Meteorological Satellite Program (DMSP) visible and near-infrared data. They used a linear interpolation between the brightest tundra and the darkest snow-covered forest and assigned "parameterized albedos" of 0.21 for complete snow cover in very dense coniferous forest and 0.80 for open tundra or farmland. Fig. 2 shows two land-cover classes given by Robinson and Kukla [27], representing their "parameterized albedos" in North America: 1) albedos from 21–40, which are black in Fig. 2, are forests, and 2) albedos from 41–80, which are white in less-dense vegetation or barren lands.

A digital comparison of Robinson and Kukla's [27] Northern Hemisphere albedo map and our seven-class land-cover map shows that areas having the lowest wintertime albedos (e.g., 21–40%) in Fig. 2 correspond closely with our forest-cover class, as shown in Fig. 1. In addition, in the continental United States, the densest forests according to Zhu and Evans [29] correspond closely to the lowest albedo areas as defined by Robinson and Kukla [27], and the taiga and maritime snow-cover classes of Sturm *et al.* [30]. Thus, by independent

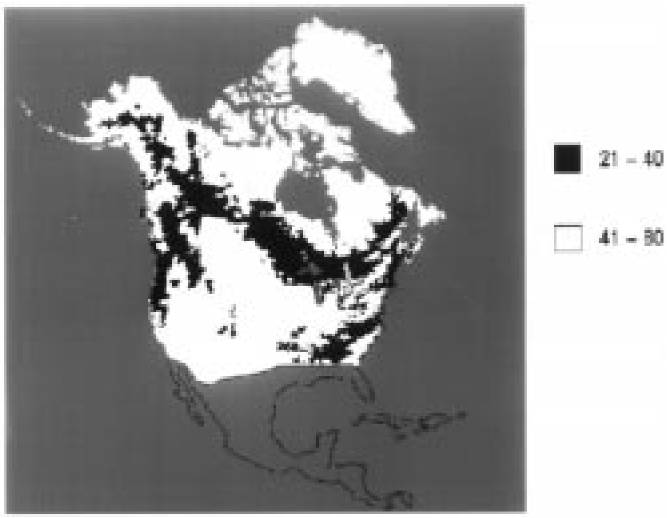


Fig. 2. Maximum surface albedo over parts of North America as derived from Defense Meteorological Satellite Program (DMSP) data by Robinson and Kukla (1985) [27]. Two categories are shown: the lowest albedos (from 21–40%, black) representing the densest forests and all other albedos combined representing other land covers (white). After Robinson and Kukla (1985) [27].

methods, location of forest cover in North America has been established, and different forest-cover densities may be identified. This information may help to determine where the snow mapping errors within forested areas will be greatest.

Foster *et al.* [25] found that the satellite-derived reflectance data in snow-covered forested regions was indicative of the actual fractional-forest cover and used the Robinson and Kukla [27] reflectance measurements as a surrogate measure for assessing the percentage of forest cover in snow-covered terrain in the Northern Hemisphere. Ponce *et al.* [31] also note a correlation between vegetation density and planetary albedo. Though NDVI, a measure of vegetation biomass, has a close relationship with the photosynthetic capacity of specific vegetation types [32], biomass is not necessarily a useful indicator of forest-cover density. Thus, the reflectance and albedo data are more useful for estimating forest cover density than is NDVI [25].

## IV. Results

*Error Estimates in "Forest" and "Mixed Agriculture and Forest":* A snow mapping error of 10% is used in this paper for *forests*, even though most of the measured errors are $< 10\%$ as determined from previous work. An additional 5% error is added to account for errors due to mixed-pixel effects at the borders of the forested areas.

The 5% error estimate due to mixed-pixel effects is based on the following. If a forest pixel (with 10% error) is next to a tundra pixel (with 0% error), then we estimate that a mixed-pixel error is 5%. Thus we estimate, empirically, that the errors in forests would average 15% under cloud-free conditions (Table III).

Snow mapping errors in the *mixed agriculture and forest* class are estimated at 5% (assuming that the class is composed equally of forest and agriculture), with an additional 5% error added for mixed-pixel effects, to provide an error of 10% in the mixed agriculture and forest class.

TABLE III
ESTIMATED SNOW MAPPING ERRORS ACCORDING TO LAND-COVER CLASS

| Land-Cover Class | Errors (%) |
|---|---|
| Mixed agriculture and forest | 10 |
| Forests | 15 |
| Barren/sparsely-vegetated | 5 |
| Tundra | 5 |
| Grassland/shrubland | 5 |
| Wetlands | 5 |
| Snow/ice | 5 |

*Error Estimates in "Nonforest" Land Covers:* Snow mapping errors in the *barren/sparsely vegetated, tundra, grassland/shrubland, wetlands, and permanent snow and ice land cover* classes north of the snowline are negligible. Though specific ground measurements have not been undertaken in all of these areas, measurements in some of the areas (e.g., tundra and grassland/shrubland) have revealed nearly 100% accuracy in measuring complete snow cover.

As was the case with the forests, an additional error of 5% is added to estimates in all classes because of expected errors at the boundaries of land-cover types due to mixed-pixel effects (Table III). Errors during snowmelt and patchy snow conditions will contribute to the total errors. However, we have undertaken only a few field measurements in patchy snow conditions [23], and thus do not have much information on snow mapping errors in patchy-snow cover. While it is important to establish snow mapping errors in patchy snow, error estimates must first be established in complete snow cover. Errors in patchy-snow cover are likely to be greater and are currently being studied [33].

*Other Snow Mapping Errors:* Studies have shown that the TM prototype algorithm correctly mapped mineral deposits around Mono Lake, CA, as nonsnow-cover. Furthermore, actual MODIS-derived maps show that we do not misidentify deserts (e.g., the Sahara) as snow cover. However, early MODIS data show some scattered nonsnow pixels misidentified as snow, and these pixels are being studied.

### *A. Monthly Snowline Positions*

Average monthly snowline positions in North America and Eurasia are reported by NOAA/NESDIS on their Northern Hemisphere weekly snow-cover maps. In Fig. 3, the average monthly snowline positions are shown for the months of January, April, July, and October for North America and Eurasia. The land-cover classes are seen north of the average continental snowline for each month.

To determine an error for North America for the month of January, the following formula may be applied:

$$\mathbf{E_{JAN}} = \mathbf{E}_{\mathrm{LC}} \sum_{\mathbf{i=1}}^{\mathbf{7}} \mathbf{A} \tag{1}$$

where $E_{JAN}$ is the average January snow mapping error, $E_{\mathrm{LC}}$ is the error in each of the seven land-cover classes (from Table III), and $A$ is the percent area of each land-cover type above the snowline in January in this case (from Table IV). Each of the monthly errors may be calculated in this way. Monthly errors

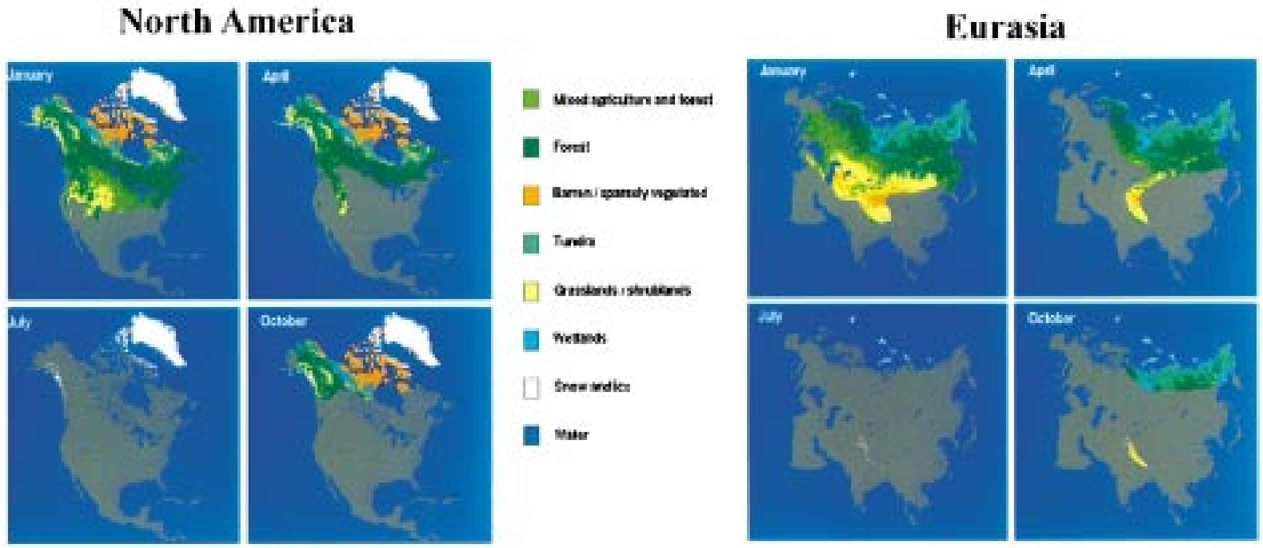


Fig. 3. Land cover (from Fig. 1) north of the average monthly snowline for four months both in North America and Eurasia.

may then be averaged to derive an estimate of an average annual error.

### B. Expected Preliminary Snow Mapping Errors

On the basis of these preliminary data, the greatest errors in snow mapping can be expected from November through April (9–10%), as shown in Fig. 4. It is during those months that snow covers most or all of the boreal forests and most of the forests located in the midcontinent regions. Though the snowline begins to retreat northward by March/April, snow cover in forests lasts longer than it does in open areas. In April, with snow still remaining in the forests, and a smaller total snow-covered area, both in North America and Eurasia, the percentage of snow in forests is high (39% and 45%, respectively) (Table IV), and the error contribution of the forests is significant.

As estimated in this work, the aggregated, Northern Hemisphere snow mapping error (in the absence of cloud cover) is about 8% and is largely determined by the percentage of forest that is snow covered in a given month.

## V. Discussion and Conclusion

This work has shown that hemispheric errors resulting from satellite snow mapping vary depending on the position of the snowline and the percentage of forest cover.

In order to assess the errors of global snow cover mapping using future MODIS data, it is first necessary to determine the errors in mapping snow in individual land covers. Preliminary snow mapping error estimates were derived from Landsat TM satellite, MAS aircraft, and simultaneous field measurements in forested, agricultural, prairie, and tundra areas in North America using prototype MODIS snow mapping algorithms. When the ground is completely snow covered, snow mapping errors using the prototype versions of the MODIS at-launch algorithm are found to be very small ($< 1\%$) in the nonforest land covers and larger and more variable in forests.

In our seven-class land-cover map of the Northern Hemisphere, the forest-cover class corresponds very well with the

TABLE IV
Percent of Land Cover According to Class by Month North of Snowline in North America and Eurasia (Due to Rounding Errors, Total Does Not Add Up to 100% in Each Month)

North America

| | ag/forest | forest | barren | tundra | grass | wetlands | snow/ice |
|---|---|---|---|---|---|---|---|
| Jan | 12 | 37 | 13 | 7 | 15 | 2 | 15 |
| Feb | 12 | 38 | 13 | 7 | 14 | 2 | 15 |
| Mar | 9 | 39 | 14 | 7 | 14 | 2 | 16 |
| Apr | 2 | 39 | 17 | 8 | 13 | 3 | 19 |
| May | 0 | 17 | 27 | 10 | 9 | 4 | 32 |
| Jun | 0 | 2 | 37 | 3 | 6 | 2 | 51 |
| Jul | 0 | 0 | 0 | 0 | 0 | 0 | 100 |
| Aug | 0 | 0 | 0 | 0 | 0 | 0 | 100 |
| Sep | 0 | 0 | 23 | 1 | 6 | 0 | 70 |
| Oct | 0 | 18 | 27 | 9 | 9 | 4 | 32 |
| Nov | 5 | 40 | 26 | 8 | 11 | 3 | 18 |
| Dec | 10 | 38 | 14 | 7 | 13 | 2 | 16 |

Eurasia

| | ag/forest | forest | barren | tundra | grass | wetlands | snow/ice |
|---|---|---|---|---|---|---|---|
| Jan | 24 | 31 | 5 | 15 | 22 | 3 | 1 |
| Feb | 25 | 30 | 5 | 14 | 23 | 3 | 1 |
| Mar | 21 | 34 | 5 | 17 | 21 | 3 | 1 |
| Apr | 11 | 45 | 2 | 25 | 10 | 5 | 2 |
| May | 1 | 29 | 3 | 50 | 9 | 4 | 3 |
| Jun | 0 | 7 | 3 | 70 | 8 | 4 | 8 |
| Jul | 0 | 0 | 0 | 0 | 0 | 0 | 100 |
| Aug | 0 | 0 | 0 | 0 | 0 | 0 | 100 |
| Sep | 0 | 1 | 4 | 43 | 4 | 1 | 48 |
| Oct | 0 | 24 | 2 | 57 | 7 | 6 | 4 |
| Nov | 14 | 41 | 3 | 24 | 12 | 4 | 2 |
| Dec | 20 | 36 | 3 | 18 | 18 | 3 | 1 |

lowest "albedos" delineated on a map of Northern Hemisphere albedo produced by Robinson and Kukla [27].

The estimated snow mapping errors for the seven land-based cover classes are 15% for the forested areas, 10% for mixed agricultural and forest areas, and 5% for each of the other five classes. The errors derived for each land cover were extrapolated to the hemispheric scale to estimate the expected monthly and

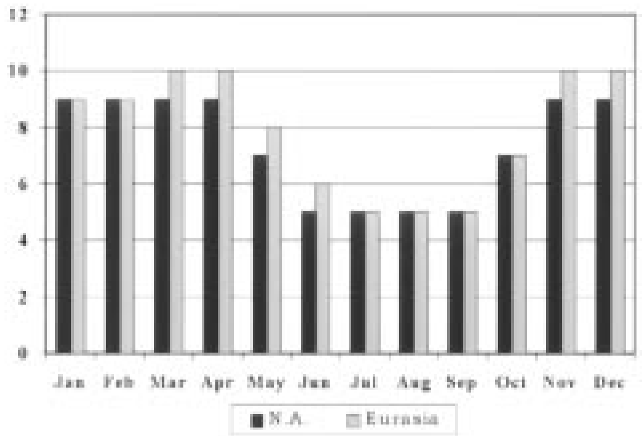


Fig. 4. Estimated errors (in %) by month for snow mapping using EOS/MODIS data for the Northern Hemisphere.

annual errors in mapping snow using MODIS snow maps. Errors are estimated to be greatest between the months of November and April in North America (9%) and Eurasia (9–10%), when snow completely covers the boreal forest. The resulting average annual snow mapping error for the Northern Hemisphere is estimated to be approximately 8%, excluding errors induced by cloud cover.

In the near future, it should be possible to use MODIS-derived reflectances in conjunction with MODIS-derived vegetation maps to delineate the densest stands within the forested areas. This will allow an improved estimate of snow mapping errors in forests to be determined.

This work has provided a technique for estimating snow mapping errors at the hemispheric scale, though actual errors cannot yet be determined. These rough error estimates will be refined about one year after MODIS data are available.

## ACKNOWLEDGMENT

The authors wish to thank Dr. D. Robinson, Rutgers University, Piscataway, NJ, for providing them with the Defense Meteorological Satellite Program (DMSP) "surface albedo" data of North America and Eurasia, and Dr. A. Strahler, Boston University, Boston, MA, for discussions about the IGBP land-cover maps. They would also like to thank Dr. C. Parkinson at NASA/GSFC, Greenbelt, MD, for her comments on the manuscript.

## REFERENCES

[1] M. Matson, C. F. Ropelewski, and M. S. Varnadore, *An Atlas of Satellite-Derived Northern Hemisphere Snow Cover Frequency*. Washington, DC: National Weather Service, 1986, p. 75.

[2] A. T. C. Chang, J. L. Foster, and D. K. Hall, "Nimbus-7 derived global snow cover parameters," *Ann. Glaciol.*, vol. 9, pp. 39–44, 1987.

[3] M. T. Hallikainen, "Retrieval of snow water equivalent from Nimbus-7 SMMR data: Effect of land-cover categories and weather conditions," *IEEE J. Oceanic Eng.*, vol. OE-9, pp. 372–376, 1984.

[4] D. K. Hall, J. L. Foster, D. L. Verbyla, A. G. Klein, and C. S. Benson, "Land and forest cover classification using aircraft and satellite data in snow-covered areas in central Alaska," *Remote Sens. Environ.*, vol. 66, pp. 129–137, 1998.

[5] A. G. Klein, D. K. Hall, and G.A. Riggs, "Improving snow-cover mapping in forests through the use of a canopy reflectance model," *Hydrol. Process.*, vol. 12, no. 10–11, pp. 1723–1744, 1998.

[6] A. Rango, "The response of areal snow cover to climate change in a snowmelt-runoff model," *Ann. Glaciol.*, vol. 25, pp. 232–236, 1997.

[7] G. E. Liston, "Interrelationships between snow distribution, snowmelt, and snowcover depletion: Implications for atmospheric, hydrologic, and ecologic modeling," *J. Climate*, to be published.

[8] Y. J. Kaufman, D. D. Herring, K. J. Ranson, and G. J. Collatz, "Earth observing system AM1 mission to Earth," *IEEE Trans. Geosci. Remote Sensing*, vol. 36, pp. 1045–1055, July 1998.

[9] W. L. Barnes, T. S. Pagano, and V. V. Salomonson, "Prelaunch characteristics of the moderate resolution imaging spectroradiometer," *IEEE Trans. Geosci. Remote Sensing*, vol. 36, pp. 1088–1100, July 1998.

[10] V. V. Salomonson, D. L. Toll, and W. T. Lawrence, "The moderate resolution imaging spectrometer (MODIS) and observations of the land surface," in *Proc. IGARSS '92 Symp.*, May 26–29, 1992, pp. 549–551.

[11] S. W. Running, C. O. Justice, V. V. Salomonson, D. K. Hall, J. L. Barker, Y. J. Kaufman, A. H. Strahler, A. R. Huete, J.-P. Muller, V. Vanderbilt, Z. M. Wan, P. Teillet, and D. Carneggie, "Terrestrial remote sensing science and algorithms planned for EOS/MODIS," *Int. J. Remote Sensing*, vol. 15, no. 17, pp. 3587–3620, 1994.

[12] C. O. Justice *et al.*, "The moderate resolution imaging spectroradiometer (MODIS): Land remote sensing for global change research," *IEEE Trans. Geosci. Remote Sensing*, vol. 36, pp. 1228–1249, July 1998.

[13] D. K. Hall, G. A. Riggs, and V. V. Salomonson, "Development of methods for mapping global snow cover using Moderate Resolution Imaging Spectroradiometer (MODIS) data," *Remote Sens. Environ.*, vol. 54, pp. 127–140, 1995.

[14] G. A. Riggs, D. K. Hall, and V. V. Salomonson, "Recent progress in development of the moderate resolution imaging spectroradiometer snow cover algorithm and product," in *Proc. Int. Geoscience and Remote Sensing Symp. '96*, Lincoln, NE, 1996, pp. 139–141.

[15] G. R. Scharfen, D. K. Hall, S. J. S. Khalsa, J. D. Wolfe, M. C. Marquis, G. A. Riggs, and B. McLean, "Accessing the MODIS snow and ice products at the NSIDC DAAC," in *Proc. Int. Geoscience and Remote Sensing Symp. '00*, Honolulu, HI, July 23–28, 2000.

[16] S. A. Ackerman, K. I. Strabala, W. P. Menzel, R. A. Frey, C. C. Moeller, and L. E. Gumley, "Discriminating clear-sky from clouds with MODIS," *J. Geophys. Res.*, to be published.

[17] T. R. Carroll, "Operational airborne and satellite snow cover products of the National Operational Hydrologic Remote Sensing Center," in *Proc. 47th Eastern Snow Conf.*. Bangor, ME, June 7–8, 1990.

[18] N. C. Grody and A. N. Basist, "Global identification of snowcover using SSM/I measurements," *IEEE Trans. Geosci. Remote Sensing*, vol. 34, pp. 237–249, Jan. 1996.

[19] M. D. King and W. P. Menzel *et al.*, "Airborne scanning spectrometer for remote sensing of cloud, aerosol, water vapor, and surface properties," *J. Atmos. Ocean. Technol.*, vol. 13, no. 4, pp. 777–794, 1996.

[20] A. G. Klein, D. K. Hall, and K. Seidel, "Algorithm intercomparison for accuracy assessment of the MODIS snow-mapping algorithm," in *Proc. 55th Eastern Snow Conf.*, Jackson, NH, June 3–5, 1998, pp. 37–45.

[21] A. B. Tait, D. K. Hall, J. L. Foster, and A. T. C. Chang, "Detection of snow cover using millimeter-wave imaging radiometer (MIR) data," *Remote Sens. Environ.*, vol. 68, pp. 53–60, 1999.

[22] K. J. Bayr, J. C. Goumas, and K. A. Picard, "Description of snow measurements—February 9, 1997, Keene, New Hampshire area: Tenant Swamp, Spofford Lake and Bretwood Golf Course," Int. Rep., Dept. Geogr., Keene State College, Keene, NH, 1998.

[23] D. K. Hall, A. B. Tait, J. L. Foster, A. T. C. Chang, and M. Allen, "Intercomparison of satellite-derived snow-cover maps," *Ann. Glaciol.*, to be published.

[24] T. R. Loveland and A. S. Belward, "The IGBP-DIS global 1 km land cover data set, DESCover: First results," *Int. J. Remote Sensing*, vol. 18, no. 15, pp. 3289–3295, 1997.

[25] J. L. Foster, A. T. C. Chang, and D. K. Hall, "Snow mass in boreal forests derived from a modified passive microwave algorithm," in *Multispectral and Microwave Sensing of Forestry, Hydrology, and Natural Resources*, E. Mougin, K. J. Ranson, and J. A. Smith, Eds. Rome, Italy, Sept. 26–30, 1994, pp. 605–617.

[26] A. T. Chang, J. L. Foster, D. K. Hall, B. E. Goodison, A. E. Walker, J. R. Metcalfe, and A. Harby, "Snow parameters derived from microwave measurements during the BOREAS winter field campaign," *J. Geophys. Res.*, vol. 102, no. D4, pp. 29 663–29 671, 1997.

[27] D. A. Robinson and G. Kukla, "Maximum surface albedo of seasonally snow-covered lands in the Northern Hemisphere," *J. Climate Appl. Meteorol.*, vol. 24, pp. 402–411, 1985.

[28] D. A. Robinson and G. Kukla, "Albedo of a dissipating snow cover," *J. Climate Appl. Meteorol.*, vol. 23, pp. 1626–1634, 1984.

[29] Z. Zhu and D. L. Evans, "U. S. forest types and predicted percent forest cover from AVHRR data," *Int. J. Remote Sensing*, vol. 60, no. 5, pp. 525–529, 1994.

[30] M. Sturm, J. Holmgren, and G. E. Liston, "A seasonal snow cover classification system for local to regional applications," *J. Climate*, vol. 8, no. 5, pp. 1261–1283, 1995.

[31] V. M. Ponce, A. K. Lohani, and P. T. Huston, "Surface albedo and water resources: Hydroclimatological impact of human activities," *J. Hydrol. Eng.*, vol. 2, no. 4, pp. 197–203, 1997.

[32] J. R. G. Townshend, C. J. Tucker, and S. N. Goward, "Global vegetation mapping," in *Atlas of Satellite Observations Related to Global Change*, R. J. Gurney, J. L. Foster, and C. L. Parkinson, Eds. London, U.K.: Cambridge Univ., 1993, pp. 301–311.

[33] J. C. Shi, "1999 progress report: Validation snow extent product from MODIS data," Progress Rep. to NASA, ICESS, Univ. California, Santa Barbara, 1999.

**Dorothy K. Hall** received the Ph.D. degree in geography from the University of Maryland, College Park, in 1980.

She has been with the Hydrological Sciences Branch, NASA/Goddard Space Flight Center, Greenbelt, MD, since 1975. She is the Associate Team Member for the Earth Observing System (EOS)/Moderate Resolution Imaging Spectroradiometer (MODIS) Snow and Ice Project. In that capacity, she manages the development of algorithms to map snow and sea ice using MODIS data. She is also a Principal Investigator on an ENVISAT synthetic aperture radar (SAR) project and a Co-Investigator of a science education project. She has been an Investigator for Landsat TM and ERS-1 and -2 SAR projects, as well as other snow, glacier, and lake ice projects. In addition to the MODIS snow research, she investigates the mass-balance changes of glaciers in Alaska, Iceland, and the Austrian Alps using SAR and Landsat data.

Dr. Hall is Past-President of the Eastern Snow Conference and a Member of the American Geophysical Union and the International Glaciological Society.

**James L. Foster** was born in Washington, DC. He received the B.S. and M.S degrees from the University of Maryland, College Park, in 1969 and 1977, respectively, and the Ph.D. from the University of Reading, Reading, U.K., in 1995.

He has been with the Goddard Space Flight Center, Greenbelt, MD, since 1973, and has been with NASA, Washington, DC, since 1978. His professional interests include the remote sensing of snow using sensors in different wavelengths, global determination of snow cover and snow mass, the influence of snow on climate, and the contribution of melting snowpacks to water supply.

Dr. Foster is a member of the American Meteorological Society and the Eastern Snow Conference, of which he served as President from 1988 to 1989. His research projects and field work have taken him to Antarctica, Greenland, Norway, Canada, as well as Alaska and the northern and mountainous states in the contiguous U.S.

**Vincent V. Salomonson** (SM'92–F'98) received the B.S. degree in agricultural engineering and the Ph.D. degree in atmospheric science from Colorado State University, Fort Collins, in 1959 and 1968, respectively, the B.S. degree in meteorology from the University of Utah, Salt Lake City, in 1960, and the M.S. degree in agricultural engineering from Cornell University, Ithaca, NY, in 1964.

He is currently the Director of the Earth Sciences Directorate with NASA's Goddard Space Flight Center, Greenbelt, MD, and is the Science Team Leader for MODIS.

Dr. Salomonson is a Fellow of the American Society for Photogrammetry and Remote Sensing (ASPRS). From 1991 to 1997, he was a member of the Executive Administrative Committee for the IEEE Geoscience and Remote Sensing Society, and he was the General Chairman of the International Geoscience and Remote Sensing Symposium (IGARSS-90), held in Washington, D.C., in May 1990. He has served the ASPRS as the Vice President, President-Elect, President (1991 to 1992), and Past-President. He is also a Member of the American Meteorological Society and the American Geophysical Union.

**Andrew G. Klein** received the B.A. from Macalester College, St. Paul, MN, and the Ph.D. from Cornell University, Ithaca, NY, in 1997.

From 1996 to 1998, he collaborated with scientists in the Hydrological Sciences Branch, NASA/Goddard Space Flight Center, Greenbelt, MD, on the development of snow cover products for the Terra MODIS instrument. He is currently an Assistant Professor in the Department of Geography, Texas A&M University, College Station, where he continues his cryospheric remote sensing studies and is involved in development of environmental monitoring programs in polar regions.

**J. Y. L. Chien** received the B.A. in mathematics from Anderson College, Anderson, IN, in 1965 and the M.S. in mathematics and statistics from Purdue University, West Lafayette, IN, in 1967 .

She is currently a Computer Programmer/Analyst with General Sciences Corporation/SAIC, Laurel, MD, working in the areas of remote sensing, scientific programming, and image processing applications. Currently, she provides technical support for the MODIS snow and ice project at Goddard Space Flight Center/NASA, Greenbelt, MD.